Physicochem. Probl. Miner. Process. 53(2), 2017, 1119−1132

www.minproc.pwr.wroc.pl/journal

Physicochemical Problems of Mineral Processing

ISSN 1643-1049 (print)
ISSN 2084-4735 (online)

Received June 1, 2016; reviewed; accepted November 25, 2016

Flotation separation of cervantite from quartz

Jinming Wang[*], Yuhua Hua[**], Shilei Yu[***], Junhui Xiao[****], Longhua Xu[****], Zhen Wang[****]

[*] Southwest University of Science and Technology, Key Laboratory of Solid Waste Treatment and Resource Recycle Ministry of Education, China. Corresponding author: wjmyutian@126.com (Jinming Wang)
[**] Central South University, Changsha, Hunan, China
[***] TianJin Huakan Ming investment Co., Ltd, China
[****]Southwest University of Science and Technology, Mianyang, Sichuan, China

Abstract: Flotation separation of cervantite (Sb_2O_4) from quartz was investigated using dodecylamine (DDA) as a collector. Experiments were conducted on single minerals and on a synthetic mixture of quartz and cervantite. Flotation separation mechanisms were investigated using the zeta potential technique, solution chemistry principles, density functional calculations and Fourier Transform Infrared (FT-IR) spectroscopy. The results indicated that DDA, primarily in the form of molecules, exhibited excellent performance in flotation of cervantite and quartz at pH 10.5. The adsorption energy of the DDA molecules on the cervantite surface was greater than the adsorption energy of water molecules, while the adsorption energy of DDA on the quartz surface was less than the adsorption energy of water molecules. DDA molecules can be adsorbed on the quartz surface to a certain extent, but it was difficult for the same molecule to be adsorbed on the cervantite surface in the pulp. This resulted in flotation of quartz. DDA molecules were adsorbed on quartz not only through physical adsorption but also by hydrogen bonding. However, cervantite could not be floated at pH 10.5 since adsorption of DDA molecules occurred through weak physical bonds on cervantite.

Keywords: *cervantite, quartz, dodecylamine, flotation, density functional theory*

Introduction

Antimony, with its wide range of applications, has tremendous importance in various industries, including production of flame retardants, processing of alloys to increase hardness and mechanical strength of other metals, as well as production of bullets (Anderson, 2012). Currently, antimony sulphides are used as the primary sources of antimony. It is relatively easier to separate sulphide minerals from the gangue using conventional flotation (Ou et al., 1998; Riaz et al., 2008). However, with the depletion of antimony sulphides (Henckens et al., 2016) beneficiation of oxide type antimony

http://dx.doi.org/10.5277/ppmp170234

ores has recently gained importance. Cervantite (Sb_2O_4), is one of the most important antimony oxides. Quartz (SiO_2) occurs as the main gangue mineral. Owing to the similarities in the physicochemical and surface chemistry features, separation of cervantite from quartz by flotation is challenging. Dodecylamine (DDA) is an effective collector for oxide ores and is widely used in flotation of zinc oxides, bauxite, collophane and rejection of silicates from iron ores through reverse flotation (Majid et al., 2011; Filippov et al., 2014; Liu et al., 2015a, 2015b). However, DDA, as the collector in cervantite flotation, has not been previously studied. A number of researchers (Han et al., 2016; Chen et al., 2015) have successfully used density functional calculations (DFT) to explain adsorption phenomenon for some minerals and reagents. However, no DFT study on adsorption of reagents on cervantite exists in the literature.

In this work, separation of cervantite from quartz through flotation was investigated using DDA as the collector. The solution chemical analysis, adsorption studies, FTIR analysis and DFT calculations were performed to investigate and explain DDA interaction with quartz and cervantite.

Materials and methods

Minerals and reagents

Bulk samples of cervantite and quartz were obtained from the Xikuangshan in Hunan, China. Both samples were crushed by hammering and high purity crystals were manually separated using a microscope. The samples were then dry-ground in a porcelain ball mill and were wet-screened using distilled water to obtain -0.074+0.038 mm fraction. For FTIR analysis and zeta potential measurements, -0.038 mm samples were further ground to approximately -0.005 mm. Quartz samples were treated with dilute hydrochloric acid (HCl) to remove any impurities. Then, quartz samples were washed several times with distilled water. The purity of quartz and cervantite particles was over 90% based on the X-Ray diffraction and chemical analysis.

Analytical grade DDA was purchased from Guangfu, Tianjin. DDA was prepared by mixing equimolar amounts of DDA and acetic acid (CH_3COOH). Solutions of HCl and NaOH were used to adjust the pH of the system and distilled water was used throughout the experiments.

Flotation tests

Flotation tests for both single mineral (cervantite and quartz) and mixtures of minerals (2 g) were conducted in a XFG flotation machine using a 40 cm^3 flotation cell, at an impeller speed of 1800 rpm. The mixture of minerals was prepared by mixing cervantite and quartz at a mass ratio of 1:1,. The reagents were added in the following order: (a) HCl or NaOH conditioning for 3 min; (b) DDA (1.5×10^{-4} mol·dm^3) conditioning for 3 min. A frother was not used in the flotation tests because of the

frothing action of DDA. Next, the pulp was agitated for three minutes and the pH was measured before flotation. After 3 minutes of flotation, the froth (F) and tailing products (T) were collected, dried and weighed separately. Results were given as weight recovery (*R*, %) of floated minerals, calculated according to the formula:

$$R\,(\%) = \frac{\mathrm{F}}{\mathrm{F}+\mathrm{T}} \times 100\% \,. \tag{1}$$

Zeta potential measurements

Zeta potentials of minerals were measured with a JS94H zeta potential analyzer (Jiang et al., 2012). The mineral samples used for this purpose were ground to finer than 5 μm in an agate mortar and pestle. Mineral samples below 5 μm (20 mg) were added to the 40 cm^3 aqueous solution with and without 1.5×10^{-4} $mol\cdot dm^3$ DDA and stirred for 5 minutes. Then, the pH values were adjusted and measured. The colloid suspension was transferred to an electrophoresis vessel. The electrodes of the micro-electrophoresis meter were wetted previously to avoid any disturbance due to air bubbles. The migration of the colloidal particles under a potential gradient of 10 V cm^{-1} was observed on the computer monitor through a camera and a multimedia system. An average of the electrophoretic velocity was obtained by the computer by considering the motion of 10 particles, first in one direction and next in the opposite direction obtained by reversal of the polarity of the applied electrical field. The zeta potential values were calculated using the software. The results presented are the averages of three independent measurements.

FTIR measurements

The infrared spectra of samples were recorded by a Nicolet 6700 spectrometer at ambient conditions in the range of 4000 to 500 cm^{-1}. Prior to the test, pure mineral samples were ground to -5 μm in an agate mortar prior to conditioning with the collector. Spectra of the mineral samples were retrieved using KBr pellets.

DFT calculations

Calculations were done using Cambridge Serial Total Energy Package 5.5 (CASTEP) (Payne et al., 1992), which was a first-principle pseudopotential method based on Density-Functional Theory (DFT). The exchange correlation function was a Local Density Approximation (LDA) (Ceperley and Aler 1980; Perdew and Zunger, 1981) (CA-PZ). The kinetic energy cut-off (260 eV and 290 eV) of the plane wave basis was used for cervantite and quartz, respectively, and the Brillouin zone was sampled with Monkhorst and Pack special k-points of a 2×3×1 grid for all structure calculations (Monkhorst and Pack, 1976), which showed that the cut-off energy and the *k*-point meshes were sufficient for the system. For self-consistent electronic minimization, the Pulay Density Mixing method was employed with the convergence tolerance of

2.0×10^{-6} eV·atom^{-1}. The energy tolerance was 2.0×10^{-5} eV·atom^{-1}, the force tolerance was 0.05 eV·Å^{-1}, and the displacement tolerance was 0.002 Å (0.0002 nm).

The cervantite structure crystallizes in space group *P*bn2_1 with the cell parameter of a = 5.456 Å, b = 4.814 Å, c = 11.787 Å and $\alpha = \beta = \gamma = 90°$ (Orosel et al., 2005). The quartz structure crystallizes in space group $P3_121$, with the cell parameter of a = b = 4.913 Å, c = 5.405 Å and $\alpha = \beta = 90°$, $\gamma = 120°$ (Glinnemann, 1992). Theoretical methods showed that cervantite and quartz (001) surfaces underwent considerable relaxation which resulted in a low surface free energy. The optimizations of water molecular, DDA ion and DDA molecule were calculated in a 10×10×10 Å cubic cell, and the optimizations were performed at the gamma point in the Brillouin zone.

The construction of the cervantite and quartz (001) plane was as follows: the first step was to optimize the primitive cell. The second step was to cleave a nine atomic-layer slab of cervantite (001) plane and an eighteen atomic-layer slab of quartz (001) plane based on the optimized primitive cell, and then create a 2×2×1 super cell. The thickness of the vacuum slab was 20 Å (2 nm). Finally, the geometric optimization of the cervantite and the quartz (001) plane was performed. In the optimized lattice, after geometric optimization, water molecular, DDA ion and DDA molecule were positioned on the cervantite and quartz (001) surface at various possible adsorption sites. The adsorption energy could be expressed by equation:

$$E_{ads}=E_{(surface/adsorbate)}-E_{surface}-E_{adsorbate} \quad (2)$$

where E_{ads} is the adsorption energy, $E_{(surface/adsorbate)}$ is the total interaction energy of the adsorbate with the mineral surface in the equilibrium state, $E_{surface}$ is the energy of the mineral surface, and $E_{adsorbate}$ is the energy of the adsorbent. According to this definition, a negative value represents an exothermic process and the greater the value, the stronger the adsorption interaction between the adsorbate and the substrate.

Results and discussion

Flotation performance of single minerals

Figure1 shows flotation recoveries of cervantite and quartz as a function of pH in the presence of DDA (1.5×10^{-4} mol·dm^3). The recovery of cervantite reaches over 90% under the conditions of pH 2 to 8 and decreases sharply when the pH increases to 10.5. When the pH is above 10.5, the recovery of cervantite is approximately 10%. The recovery of quartz increases with the increase in pH from pH 2 to the maximum (95%) at approximately pH 6 and subsequently levels off at the pH range of 6 to 12. Thus, it could be concluded that the pulp pH should be either highly acidic (pH<2) or highly alkaline (pH>10.5) for separation of cervantite from quartz. However, it is a challenge to precisely adjust pulp pH to acidic conditions in the practical scale since the ore consists of alkaline gangue such as carbonaceous minerals. Therefore, in this work,

alkaline conditions were used. The difference in the flotation recoveries of quartz and cervantite is over 70% at pH 10.5 when reverse flotation was performed.

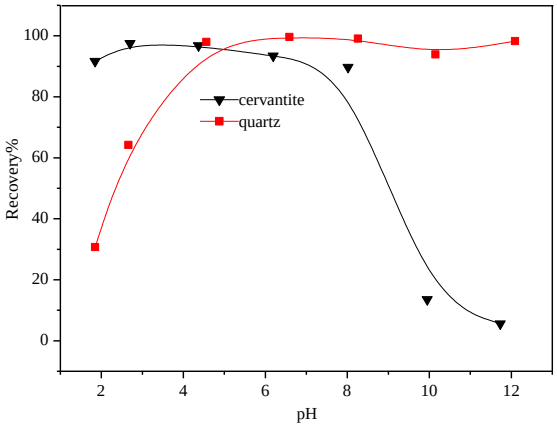

Fig. 1. Effect of pH on recovery of minerals using DDA as the collector

The effect of DDA concentration on flotation of the two minerals, as shown in Fig. 2, further ensures the outstanding selectivity of DDA. At pH 10.5, floatability of quartz increases with an increase in the collector concentration. When the collector concentration is 1.5×10^{-4} mol·dm^3, flotation recovery is almost maximum. When the recovery of quartz approaches approximately 95%, the recovery of cervantite is only 23.8%. This implies that DDA has a good selectivity and a high collecting capacity, which is suitable for separating cervantite from quartz at a pulp pH of 10.5 at the DDA concentration of 1.5×10^{-4} mol·dm^3.

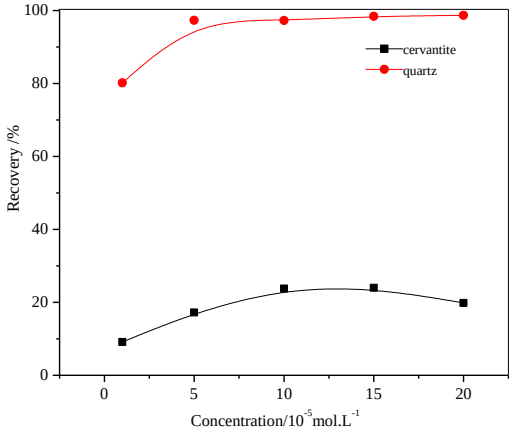

Fig. 2. Effect of DDA concentration on recovery of minerals at pH 10.5

Flotation of the synthetic quartz-cervantite mixture

The results of single mineral flotation tests (Fig. 3) show that DDA has an excellent ability to separate cervantite from quartz at pH 10.5. Further, flotation tests on the synthetic mixture of quartz and cervantite were carried out. The mixture was prepared by blending quartz and cervantite at a mass ratio of 1:1, that is, the mixtures contained 39.51% Sb. The results of flotation tests as a function of pH are presented in Fig. 3. It can be seen that separation of cervantite from quartz was achieved quite successfully: Sb recovery reached 90% and the concentrate contained 73.34% Sb at a pulp pH of 10.5. At pH>10.5, the recovery of Sb increases, while Sb grade decreases. This implies that floatability of quartz decreases with the increase in pH to a certain extent.

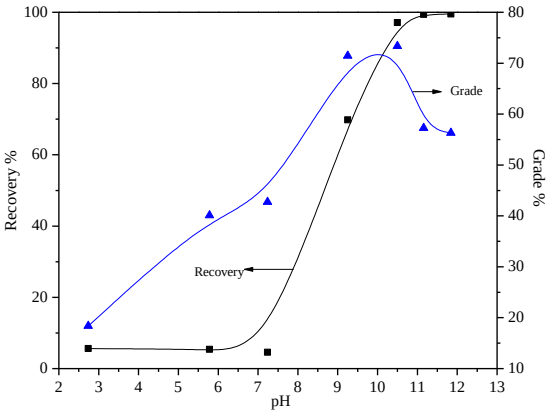

Fig. 3. Separation of cervantite from cervantite–quartz mixture (1:1) using 1.5×10^{-4} mol·dm^3 DDA

Zeta potential

To investigate the difference in the adsorption mechanism of DDA on the surfaces of two minerals, zeta potential measurements of cervantite and quartz were conducted. Zeta potential values as a function of pulp pH with and without DDA, are depicted in Fig. 4. The isoelectric points of cervantite and quartz were found as pH 2.4 and 2.6, respectively, consistent with previously reported results (Li and BruynDe, 1966; Liao, 1983; Kim and Lawler, 2005). The zeta potential of cervantite and quartz increases after adding DDA. This indicates that DDA adsorbs on the negatively charged surfaces of cervantite and quartz (Xu et al., 2015).

Figure 5 shows the relationship between pH and zeta potential (Quast, 2016) of two minerals before and after addition of DDA. As shown in Figure 5, the zeta potential difference between two minerals increases with increase in pH, implying that that DDA adsorbs more easily on the surfaces of two minerals with increasing pH. When pulp pH is higher than 10.5, zeta potential increment of cervantite is dramatically reduced, while the increment in the zeta potential quartz decreases gradually. This observation indicates that adsorption of DDA on particle surfaces becomes relatively

weaker for both minerals: Adsorption of DDA on cervantite weakens significantly while adsorption of DDA on quartz weakens at a small extent, consistent with the flotation behavior of the two minerals with DDA.

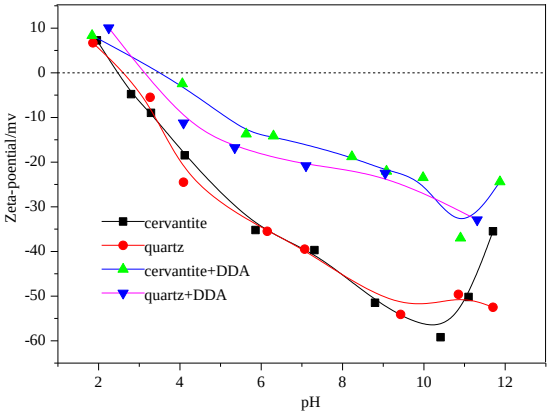

Fig. 4. Zeta potentials of cervantite and quartz with and without DDA as a function of pulp pH

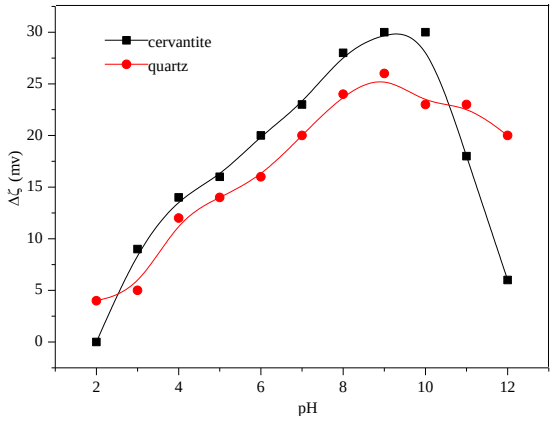

Fig. 5. pH vs. zeta potential difference (Δζ) of quartz and cervantite with and without DDA

Chemical analysis of the solution

The species distribution of DDA (Gao, 2015) at the concentration (C_T) of 1.5×10^{-4} mol·dm^3 is provided in Fig. 6. Figures 1 and 6 show that the flotation recovery of cervantite is consistent with the ionic distribution of DDA. DDA exists mainly in ionic form at pH<8, corresponding to a high flotation recovery of cervantite. The DDA ion concentration decreases, while the concentration of DDA in molecular form increases at 8<pH<10.5, corresponding to the gradual decrease in the flotation recovery of cervantite. The DDA ion concentration decreases rapidly at pH>10.5. ın pH>10.5 DDA probably occurs mainly in either molecular form or it precipitates. This pH

range also corresponds to the lowest flotation recovery of cervantite. It can be concluded that the DDA ion is the main component for collecting cervantite at pH<8. The DDA in molecular form has no collection capability for cervantite.

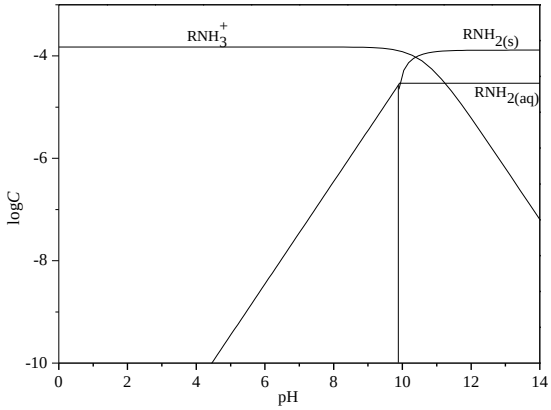

Fig. 6. Species distribution log C-pH diagram of DDA

DFT calculations

To investigate the adsorption behavior of the DDA ion, DDA molecule and water molecules on the surfaces of both minerals, the adsorption energies were computed for the (001) cleavage plane of cervantite and quartz. In the simulation process, all possible parking areas were chosen for calculation and the collector was allowed to interact with the surface. Several initial conformations were assessed to locate the minimum energy conformation of the mineral-reagent complex.

The optimized configurations of water molecule adsorption on the cervantite surface are shown in Fig. 7. Water molecules adsorb on the antimony atom atop the cervantite surface through the oxygen atom. The calculated adsorption energy is –132.44 kJ·mol^{-1}, and the equilibrium distance between the antimony atom and the oxygen atom is 2.209×10^{-10} m.

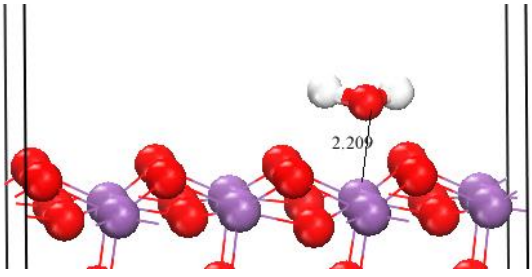

Fig. 7. The optimized adsorption configurations of H_2O on cervantite surface

The optimized configurations of DDA adsorption in ionic and molecular forms on the cervantite surface are presented in Figs. 8 (a) and (b), respectively. DDA adsorbs on the antimony atom atop the cervantite surface through the hydrogen atom of the amine group. The equilibrium distance of the DDA ion and the DDA molecule, which is adsorbed on cervantite surface, is 1.428×10^{-10} m and 1.742×10^{-10} m, respectively. At the same time, the calculated adsorption energies of the DDA ion and the DDA molecule that is adsorbed on cervantite surface are -314.92 kJ·mol^{-1} and -39.27 kJ·mol^{-1}, indicating that the DDA ion is more easily absorbed on the cervantite surface than the DDA molecule.

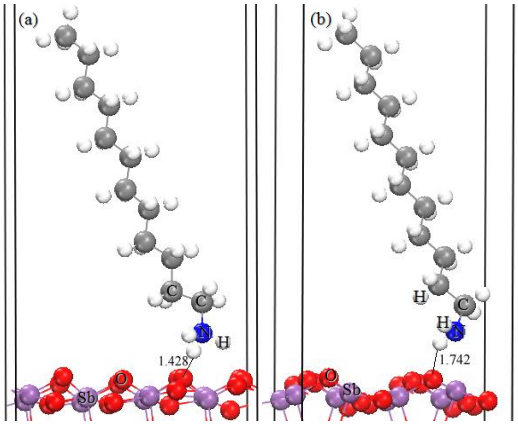

Fig. 8. The optimized adsorption configurations of the DDA ion (a) and the DDA molecule (b) on the cervantite surface

The calculated adsorption energies of the water molecule, DDA molecule and DDA ion which are adsorbed on the cervantite are provided in Table 1. The adsorption energy of three adsorbates on the cervantite surface in a descending order is: DDA molecule, water molecule and DDA ion. The adsorption energy of the water molecule is smaller than the adsorption energy of the DDA molecule, which indicates that the water molecule is absorbed on the cervantite surface more easily, forms a hydrophilic film, and prevents the DDA molecule from adsorbing on the cervantite surface. Therefore, the cervantite cannot float when DDA exists in the form of DDA molecule. The adsorption energy of the DDA cation is less than the adsorption energy of the water molecule, which indicates that the DDA cation is absorbed on the cervantite surface more easily than the water molecule and repels the hydration film formed by the water molecule on the cervantite surface. In the meantime, the DDA cation forms a hydrophobic layer on the cervantite surface to achieve cervantite flotation. Therefore, high DDA cation concentration corresponds to a high recovery of cervantite in cervantite flotation tests, and the decreasing concentration corresponds to the reduced cervantite recovery. In addition, the DDA molecule as the main component in the pulp corresponds to the lowest recovery of cervantite.

Table 1. Adsorption energy of the three adsorbates on the cervantite surface

Adsorbate	DDA Molecule	H_2O Molecule	DDA Ion
Adsorption energy ($kJ \cdot mol^{-1}$)	-39.27	-132.44	-314.92

To identify the differences in the flotation mechanism of cervantite and quartz at pH>10.5, the adsorption behavior of DDA cation, DDA molecule and water molecule on the quartz surface was studied. Figure 9 shows the optimized adsorption configuration of the water molecule on the quartz surface. The O atom of the water molecule adsorbs on the Si atom of the quartz surface, and the two H atoms of the water molecule adsorb on the O atoms of quartz. The adsorption energy is -108.98 $kJ \cdot mol^{-1}$, and the Si-O bond and the two H-O bonds have a length of 1.724×10^{-10} m, 1.612×10^{-10} m, and 1.394×10^{-10} m, respectively.

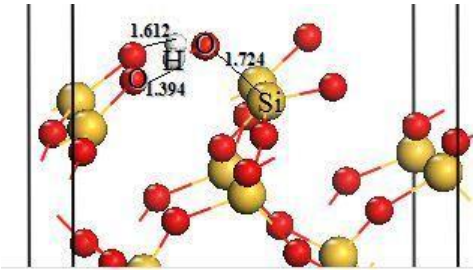

Fig. 9. Optimized adsorption configuration of H_2O on the quartz surface

Figure 10 shows the optimized adsorption configuration of the DDA cation (a) and DDA molecule (b) on the quartz surface, respectively. Both are adsorbed on the oxygen atom of the quartz surface by the hydrogen atoms of the amidogen. The adsorption equilibrium position distances between the DDA cation and the quartz, the DDA molecule and the quartz are 1.351×10^{-10} m and 1.755×10^{-10} m, respectively. The adsorption energies of the DDA cation and the DDA molecule on the surface of the quartz are -470.627 $kJ \cdot mol^{-1}$ and -177.353 $kJ \cdot mol^{-1}$, respectively.

The adsorption energy of three types of adsorbates on the quartz surface is shown in Table 2. According to Table 2, the adsorption energies in descending order of the three adsorbates on the quartz surface is H_2O, DDA and DDA^+, which shows that both dodecylamine molecule and the cation can repel the hydration film and form a hydrophobic layer on the quartz surface (Liu et al., 2015). Therefore, DDA, which is primarily in the form of a DDA molecule at pH>10.5, can be still adsorbed on the quartz surface and achieves quartz flotation at a certain concentration. The adsorption energy of the DDA molecule on the quartz surface is greater than the adsorption energy of the DDA cation, which indicates that the DDA cation is easier to adsorb on the quartz surface than the DDA molecule and corresponds to the flotation behavior of quartz with DDA as the collector. As the pH value of the pulp increases gradually,

the concentration of the DDA molecule increases, the concentration of the DDA cation decreases, and the flotation recovery of quartz is reduced.

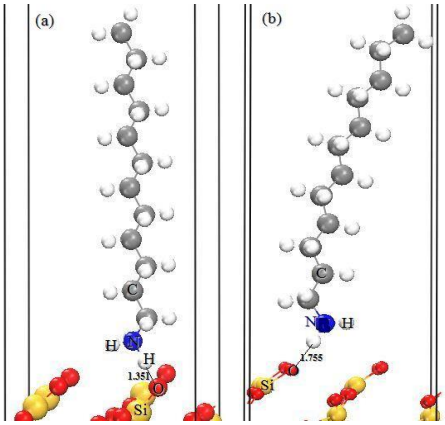

Fig. 10. Optimized adsorption configurations of the DDA ion (a) and DDA molecule (b) on the quartz surface

Table 2. Adsorption energy of three adsorbates on the quartz surface

Adsorbate	DDA molecule	H_2O molecule	DDA ion
Adsorption energy (kJ·mol^{-1})	-177.353	-108.977	-470.627

FTIR analysis

To further examine the reason for the discrepancy in the adsorption behavior of the DDA on cervantite and quartz, the infrared spectra of cervantite, quartz and these two minerals that were conditioned with DDA (1.5×10^{-4} mol·dm^3) at pH 10.5 were measured, and the results are shown in Figs. 11 and 12, respectively.

In the spectrum of DDA (Fig. 11), the characteristic sharp bands at 3331.5 cm^{-1} are the stretching vibration of the -NH group. Two peaks shown at 2921.0 and 2852.6 cm^{-1} were assigned to the –CH stretching group (Zhang et al., 2014). Three peaks at 1650.7, 1570.3 and 1487.9 cm^{-1} were assigned to the $–NH_2$ bending vibration group (Xu et al., 2015). The peak at 1154.3 cm^{-1} belongs to the –CN stretching group (Vidyadhar and Rao, 2007; Kou et al., 2010). The spectrum of cervantite treated by DDA at pH 10.5 does not exhibit the stretching vibration of the -NH group near 3331.5 cm^{-1}, which shows that the -NH group does not adsorb on the cervantite surface. Only a very weak peak of the –CH stretching group at 2925.0 cm^{-1} is observed, which means small amounts of DDA will be adsorbed on the cervantite surface at pH 10.5. The peak does not shift, which means only physical adsorption occurs, and interaction between DDA and cervantite consists mainly of the van der Waals force.

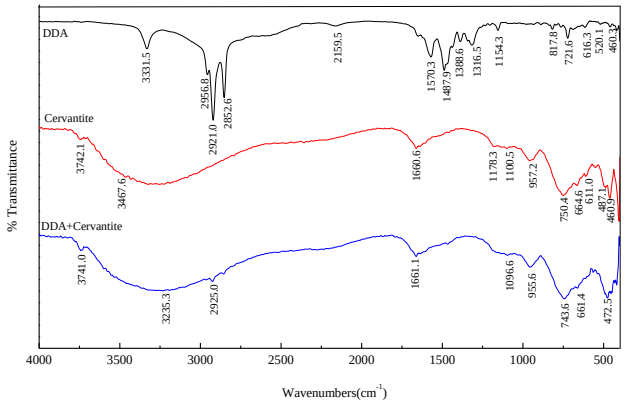

Fig. 11. FTIR spectra of (DDA, cervantite, cervantite treated by DDA) at pH 10.5

As shown in Figure 12, the spectrum of quartz treated with DDA at pH 10.5 exhibits the stretching vibration of the $–CH_2$ group near 2922.0 and 2853.1 cm^{-1}. The peaks of DDA at 3331.5 cm^{-1} corresponding to the –NH stretching vibration groups have clearly shifted to a lower frequency (3327.3 cm^{-1}) by hydrogen bonding action. It is concluded that the –NH group is involved in the adsorption process. Therefore, hydrogen bonding adsorption occurs, showing that the amine molecule adsorbs not only on the quartz surface by the van der Waals force but also by hydrogen bonding (Kou et al., 2010).

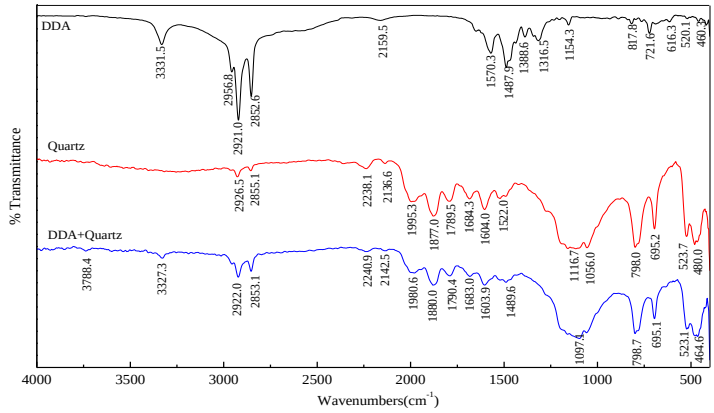

Fig. 12. FTIR spectra of (DDA, quartz, quartz treated by DDA) at pH 10.5

Conclusions

DDA exhibits selective collection for cervantite when quartz co-exists, which enables reverse flotation separation at pH 10.5. In addition, the mechanism of selective cervantite reverse flotation from quartz with DDA as the collector at pH 10.5 is clearly

distinguished. The isoelectric point of cervantite is found at pH 2.4. The zeta potential difference shows that DDA prefers to adsorb on the surface of quartz at pH 10.5. DDA is mainly in the molecular form at pH>10.5. The adsorption energy of the DDA molecule on the cervantite surface is greater than the adsorption energy of the water molecule, indicating that the cervantite cannot float when the DDA exists in the form of the DDA molecule. The adsorption energy of DDA and DDA^+ on the quartz surface is less than the adsorption energy of the water molecule, indicating that quartz can float when the DDA exists in the form of the DDA molecule and the DDA ion because the DDA molecule adsorbs on the cervantite surface by only a weak physical adsorption at pH 10.5, while on the quartz surface the DDA molecule adsorbs not only by physical adsorption but also by hydrogen bonding adsorption.

Acknowledgments

The financial supports from the Research Fund for the Doctoral Program from Southwest University of Science and Technology (14zx7131), the Opening Projects of Key Laboratory of Solid Waste Treatment and Resource Recycle, Ministry of Education (14tdgk03) and the National Natural Science Foundation of China (No. 51504199**)** are gratefully acknowledged.

References

ANDERSON, C.G., 2012, *The metallurgy of antimony,* Chem. Erde-Geochem., 72(S4), 3-8.

CEPERLEY, D. M., ALDER, B. J., 1980, *The ground state of the electron gas by a stochastic method,* Phys. Rev. Lett., 45(7), 566-569.

CHEN, J. H., KE, B. L., LAN, L. H., LI, Y. Q., 2015, *DFT and experimental studies of oxygen adsorption on galena surface bearing Ag, Mn, Bi and Cu impurities,* Miner. Eng., 71, 170-179.

FILIPPOV, L.O., SEVEROV, V.V., FILIPPOVA, I.V., 2014, *An overview of the beneficiation of iron ores via reverse cationic flotation,* Int. J. Miner. Process., 127, 62-69.

GLINNEMANN, J., 1992, *Crystal structures of the low-temperature quartz-type phases of SiO_2 and GeO_2 at elevated pressure,* Z. Kristallogr. Krist., 198(3-4), 177-212.

GAO, Z. Y., SUN, W., HU, Y. H., 2015, *New insights into the dodecylamine adsorption on scheelite and calcite: An adsorption model,* Miner. Eng., 79, 54-61.

HAN, Y. H., LIU, W. L., CHEN, J. H., 2016, *DFT simulation of the adsorption of sodium silicate species on kaolinite surfaces,* Appl. Surf. Sci., 370, 403-409.

HENCKENS, M.L.C.M., DRIESSEN, P.P.J., WORRELL, E., 2016, *How can we adapt to geological scarcity of antimony? Investigation of antimony's substitutability and of other measures to achieve a sustainable use,* Resour. Conserv. Recy.,, 108, 54-62.

JIANG, T.Y., JIANG, J., XU, R. K., LI, Z., 2012, *Adsorption of Pb (II) on variable charge soils amended with rice-straw derived biochar,* Chemosphere, 89(3), 249-256.

JUANG, R.S., WU, W. L., 2002, *Adsorption of Sulfate and Copper (II) on Goethite in Relation to the Changes of Zeta Potentials,* J. Colloid Interf. Sci., 249(1), 22-29.

KIM, J. K., LAWLER, D. F., 2005, *Characteristics of zeta potential distribution in silica particles,* B. Kor. Chem. Soc., 26(7), 1083-1089.

KOU, J., TAO, D., XU, G., 2010, *A study of adsorption of dodecylamine on quartz surface using quartz crystal microbalance with dissipation,* Colloid. Surface. A, 368, 75-83.

LIU, A., FAN, J.C., FAN, M. Q., 2015a, *Quantum chemical calculations and molecular dynamics simulations of amine collector adsorption on quartz (0 0 1) surface in the aqueous solution,* Int. J. Miner. Process., 134, 1-10.

LIU, J., WANG, X. M., LIN, C. L., MILLER, J.D., 2015b, *Significance of particle aggregation in the reverse flotation of kaolinite from bauxite ore,* Miner. Eng., 78, 58-65.

LI, H. C., DE BRUYN, P. L., 1966, *Electro-kinetic and adsorption studies on quartz,* Surf. Sci., 5(2), 203-220.

LIAO, P. J., 1983, *Study on surface electrical properties and floatability of antimony oxide,* J. Cent. S. I. Min. Metall., 1, 21-29.

MAJID, E., MEHDI, I. MAHDI, G., 2011, *Influence of important factors on flotation of zinc oxide mineral using cationic, anionic and mixed (cationic/anionic) collectors,* Miner. Eng., 24(13):1402-1408.

MONKHORST, H.J., PACK, J.D., 1976, *Special points for Brillouin-zone integrations,* Phys. Rev. B, 13(12), 5188- 5192.

OROSEL, D., BALOG, P., LIU, H., QIAN, J., JANSEN, M., 2005, *Sb_2O_4 at high pressures and high temperatures,* J. Solid State Chem., 178(9), 2602-2607.

OU, L. M., FENG, Q. M., CHEN, J., 1998, *The pulp electrochemistry of flotation separation for stibnite-arsenopyrite bulk concentrate,* J. Cent. S. Univ. Tec., 5(1), 4-6.

PAYNE, M.C., TETER, M.P., ALLAN, D.C., ARIAS, T.A., JOANNOPOULOS, J.D., 1992, *Iterative minimization techniques for ab initio total energy calculation: molecular dynamics and conjugate gradients,* Rev. Mod. Phys., 64(4), 1045-1097.

PERDEW, J. P., ZUNGER, A., 1981, *Self-interaction correction to density-functional approximations for many- electron systems,* Phys. Rev. B, 23(10), 5048-5079.

QUAST, K. 2016, *The use of zeta potential to investigate the interaction of oleate on hematite,* Miner. Eng., 85, 130-137.

RIAZ, M., JAN, N., HUSSAIN, M., KHAN, F., YAMIN, A., 2008, *Flotation studies of low grade stibnite ore from Krinj (Chitral) area,* J. Chem. Soc. Pakistan, 30(4), 584-587.

VIDYADHAR, A., RAO, H.K., 2007, *Adsorption mechanism of mixed cationic/anionic collectors in feldspar-quartz flotation system,* J. Colloid Interf. Sci., 306(2), 195-204.

XU, S. H., KOU, J., SUN, T. C., JONG, K., 2015, *A study of adsorption mechanism of dodecylamine on sphalerite,* Colloid. Surface. A, 486, 145-152.

ZHANG, S., LIU, Q. F., CHENG, H. F., LI, X. G, ZENG, F. G., FROST, R.L., 2014, *Intercalation of dodecylamine into kaolinite and its layering structure investigated by molecular dynamics simulation,* J. Colloid Interf. Sci., 430, 345-350.